THE JOURNAL OF PHYSICAL CHEMISTRY A

 VOLUME 105, NUMBER 47, NOVEMBER 29, 2001

FEATURE ARTICLE

Mass and Thermal Accommodation Coefficients of $H_2O(g)$ on Liquid Water as a Function of Temperature

Y. Q. Li and P. Davidovits*

Chemistry Department, Merkert Chemistry Center, Boston College, Chestnut Hill, Massachusetts 02467-3809

Q. Shi, J. T. Jayne, C. E. Kolb, and D. R. Worsnop

Center for Aerosol and Cloud Chemistry, Aerodyne Research, Inc., Billerica, Massachusetts 01821-3976

Received: July 17, 2001; In Final Form: September 26, 2001

The probabilities that a water vapor molecule striking a liquid water surface will (1) thermally equilibrate with the liquid surface and (2) penetrate that surface and be incorporated into the bulk liquid are parameters of fundamental importance to both chemical physics and atmospheric science. Here we report values for these parameters as a function of temperature in the range of 258−280 K, measured with a droplet train flow reactor under conditions that circumvent difficulties encountered in earlier studies. The mass accommodation coefficient (α) of $H_2O(g)$ on water was determined by measuring the uptake of ^{17}O labeled gas-phase water under near equilibrium conditions. The mass accommodation coefficient has a negative temperature dependence, with the magnitude ranging from 0.17 ± 0.03 at 280 K to 0.32 ± 0.04 at 258 K. The temperature dependence and the magnitude of α are consistent with the critical complex theory of mass accommodation, previously applied to the uptake of other gas-phase species by aqueous surfaces. Experiments with $D_2O(g)$ on liquid water show that D−H isotope exchange on the liquid surface proceeds with unit probability, independent of temperature. This result implies that the thermal accommodation coefficient of $H_2O(g)$ on liquid water is 1 in the temperature range studied.

Introduction

The growth of cloud droplets and aqueous atmospheric aerosol particles is often controlled by the transfer of water vapor molecules into liquid droplets. Two parameters which fundamentally influence the interaction of water vapor or any other gaseous molecule with a liquid surface are the mass accommodation (or condensation) coefficient (α) and the thermal accommodation coefficient (S). The mass accommodation coefficient is the probability that a gaseous molecule striking a liquid surface enters into the bulk liquid phase. The thermal accommodation coefficient is the fraction of collisions that results in the kinetic and vibrational/rotational energies of the impinging gas molecule equilibrating with the mean energy of the liquid surface molecules.

The mass accommodation coefficient of water vapor on liquid water is a fundamental physicochemical parameter that has not yet been accessible to ab initio theoretical study. This kinetic parameter is important in atmospheric science, crucial to our understanding of the degree to which ambient atmospheric aerosol particles are activated to nucleate cloud droplets. Such nucleation controls the number density and size spectrum of the resulting cloud droplets in forming or evaporating clouds.[1−4] The number density of cloud droplets and their size spectrum,

* To whom correspondence should be addressed. E-mail: paul.davidovits@bc.edu.

10.1021/jp012758q CCC: $20.00
Published on Web 11/07/2001

in turn, have an important impact on atmospheric radiative transport, determining the role of clouds (and pollution driven aerosols) in both daily meteorology and climate change.[1−7]

Because of its importance, the mass accommodation coefficient of water vapor has been the subject of at least 40 published experimental studies over the past 75 years. These studies obtained results that range over 3 orders of magnitude. The first measurement of this parameter, reported in 1925 by Rideal,[8] yielded a value $\alpha = 0.003$. Prior to 1985, experiments yielded values of α ranging between ~0.001 and 1 (see reviews 9−11). More recent measurements of α, published between 1987 and 2000, still span 2 orders of magnitude, between 0.01 and 1. Specific values from recent works (with temperature stated where provided) include $\alpha = 0.01$;[12] $\alpha = 0.30$ at $T = 258$ K;[13] $0.01 \leq \alpha \leq 1$ at $T = 282-293$ K;[14] $\alpha = 0.1$ at $T = 298$ K;[15] $0.04 \leq \alpha \leq 0.1$ at $T = 238$ K;[16] and $0.01 \leq \alpha \leq 0.1$.[17] The temperature dependence of α was not established in any of these studies.

Fewer determinations of the thermal accommodation coefficient (S) for H_2O(g) on water are found in the literature. In 1935, Alty and Mackay[18] reported a value of $S = 1$. More recently values of S were measured in the range $0.1 \leq S \leq 1$ with most likely values quoted at $S = 1$[19] and $S = 0.6$.[16] Although in meteorology the thermal accommodation coefficient of air on water is likely to be the relevant parameter, S for H_2O(g) on water is important in experiments conducted under condition of high supersaturations and is certainly of fundamental interest.

The values of α (as well as S, where measured) quoted above were generally obtained either from measurements of evaporation or condensation rates from/on bulk water surfaces or from measurements of droplet (aerosol) growth rates in supersaturated environments. (Evaporation and condensation rates are connected via equilibrium considerations so that a measurement of the evaporative flux can yield a value for α.) The wide range of quoted α values is likely due to two inherent problems in these measurement techniques. First, in these experiments, the water vapor was generally not in thermal equilibrium with the liquid surface. Experimental condensation/evaporation rates were large, causing considerable heating or cooling of the liquid surface. Expressions for the measured condensation/evaporation rates must couple mass and energy fluxes, resulting in formulations that are functions of both α and S. Usually S, either for air on water or H_2O(g) on water, depending on the experiment, was assumed to be 1 and α was obtained from the best fit to the experimental data. However, the fitting of α to the experimental data obtained in such studies is not tight. For example, in a recent measurement of α, via droplet evaporation,[16] the observed rates were stated to be consistent with α between 0.04 and 0.1. Further, alternate formulations of the transport equations can change the value of α by factors of 2 or 3.[9,20]

Surface contamination has been identified as the second major source of error in the measurement of α. With smaller, newly generated droplets, Hagen et al.[14] measured α in the range of 0.2−1. However, as the size of the droplets (and therefore their age) increased, the magnitude of α decreased to less than 0.01. Although this study, and similar experiments cited in ref 14, did not identify the contaminants present, speculation centers on adsorbed organic material acting as a surfactant.

Here we present results of uptake experiments of $H_2{}^{17}O$(g) on liquid water using a droplet train flow reactor technique. This technique has been designed specifically to avoid the experimental difficulties noted above and has been used to measure mass accommodation coefficients and reactive uptake rates for a wide range of inorganic and organic gases by our group and others. (For a recent review, see Kolb et al.[21]). In this apparatus, measurements are conducted with newly formed droplets under conditions very close to liquid−vapor equilibrium. Mass accommodation coefficients are obtained from the uptake (condensation) of the gas-phase $H_2{}^{17}O$ isotope in trace amounts (but above its natural abundance). Thermal accommodation coefficients for H_2O(g) are inferred from measurements of the D−H isotope exchange probability for D_2O(g) interacting with the water surface. Measurements were conducted as a function of water droplet surface temperature in the range of 258−280 K.

The performance of a condensation or evaporation experiment to measure mass accommodation always requires that the gas phase species (in this case water vapor) be out of equilibrium with the liquid. In previous experiments, all of the water vapor was out of equilibrium with the liquid water. In the present studies, only the added trace isotopic species ($H_2{}^{17}O$ or D_2O) are out of equilibrium. Here, in the process of trace gas uptake, the overall water vapor pressure (and therefore gas−liquid equilibrium) are perturbed by a factor less than 10^{-3}.

In the droplet train experiments, newly formed droplets transit through the apparatus in less than 50 ms. In this way, the liquid surface is continuously renewed and remains free of contaminants. Furthermore, as discussed, the net mass and heat transfer to the liquid is negligible. Therefore, the experimental problems associated with the previous studies are circumvented.

Gas−Liquid Interactions

In the absence of surface reactions, the mass accommodation coefficient limits the maximum flux, J, of gas into a liquid, which is given by

$$J = \frac{n_g \bar{c} \alpha}{4} \tag{1}$$

Here, n_g is the molecular density of the gas molecules of interest and $\bar{c}$ is their average thermal speed. If reactions occur at the gas−liquid interface, then the flux of species disappearing from the gas phase may exceed that given by eq 1. Of course, the flux cannot exceed the collision rate $(n_g\bar{c})/4$.

In experiments on the uptake of H_2O(g), the net flux is limited by two additional effects. First, as the gas molecules enter the liquid, new molecules have to move toward the liquid surface to replenish the gas-depleted region near the liquid surface. The rate of transport toward the liquid surface is determined by gas-phase diffusion that can limit the rate of uptake by the liquid. Second, as the $H_2{}^{17}O$(g) species enters the bulk liquid, a fraction evaporates back into the gas phase. This process is governed by $H_2{}^{17}O$ gas/liquid partitioning. In experiments subject to all these effects, the measured flux (J_{meas}) into a surface may be expressed in terms of a measured uptake coefficient, γ_{meas}, that takes into account these effects:

$$J_{meas} = \frac{n_g \bar{c} \gamma_{meas}}{4} \tag{2}$$

To a good approximation, these effects can be decoupled, and γ_{meas} can be expressed as[22]

$$\frac{1}{\gamma_{meas}} = \frac{1}{\Gamma_{diff}} + \frac{1}{\alpha} + \frac{1}{\Gamma_{sol}} \tag{3}$$

Here, Γ_{diff} represents the effect on uptake when gas phase diffusive transport does not fully keep up with the rate of trace gas uptake into the liquid. The term Γ_{sol} takes into account evaporation of trace gas molecules that have entered the bulk liquid phase (i.e., Γ_{sol} represents the effect of $H_2{}^{17}O$ gas/liquid partitioning). For water, Γ_{sol} can be approximated by the expression used and validated in our previous studies:[22]

$$\frac{1}{\Gamma_{sol}} = \frac{\bar{c}}{8RTH\sqrt{\frac{\pi t}{D_l}}} \quad (4)$$

where D_l is the liquid-phase diffusion coefficient of water molecules in water ($D_l = 2.51 \times 10^{-5}$ cm^2 s^{-1} at 25 °C), t is the gas−liquid interaction time, R is the gas constant in units L atm/(K mol), T is temperature, and H (M atm^{-1}) is the Henry's law constant. Note that Γ_{sol} measures the extent to which the gas-phase species is out of equilibrium with the liquid. As equilibrium is approached, Γ_{sol} approaches 0.

The expression for Γ_{sol} in eq 4 was derived to take into account the effect of solubility limitations for a trace gas entering water. In that case, H is the well-defined Henry's law constant. The form of eq 4 is expected to be valid also for the uptake of gas-phase water into water. However, it is not clear how to obtain a value of H to be used in this case. We propose here to identify H as the gas/liquid partitioning constant defined in terms of the molarity [H_2O(aq)] of liquid water and its equilibrium vapor pressure (p_{H2O}) as

$$[H_2O(aq)] = Hp_{H_2O} = [H_2O(g)]RTH \quad (5)$$

The use of eq 5 to calculate H is reasonable but has not been validated. Therefore, Γ_{sol} as calculated via eqs 4 and 5 provides a guide but not a firm treatment of solubility limitations on the uptake of H_2O(g).

Gas-phase diffusive transport of a trace gas to a train of moving droplets does not lend itself to a straightforward analytical solution; analytical solutions are not available even for a single stationary droplet over the full range of relevant Knudsen numbers (Kn). However, an empirical formulation of diffusive transport to a stationary droplet developed by Fuchs and Sutugin[23] has been shown to be in good agreement with measurements.[24,25]

Using the Fuchs−Sutugin formulation, Γ_{diff} is expressed as[26]

$$\frac{1}{\Gamma_{diff}} = \frac{0.75 + 0.283Kn}{Kn(1 + Kn)} \quad (6)$$

Here, $Kn = 2\lambda/d_f$; $\lambda = 3D_g/\bar{c}$ is the gas-phase mean free path; d_f is the droplet diameterand; D_g is the diffusion coefficient of the trace gas in the background gas obtained as in ref 27.

Extensive experiments have demonstrated that, with a simple modification, the Fuchs−Sutugin formulation provides a good representation of diffusive transport to a train of closely spaced, monodispersed moving droplets. In the modified expression, d_f in eq 6 is made equal to $2.0d_o$, where the d_o is the diameter of the droplet-forming orifice.[22,27−29]

Mass accommodation can be viewed as a two step process involving surface adsorption followed by a competition between desorption and solvation.[22,30] First, the gas molecule strikes the surface and is thermally accommodated. The adsorption rate constant is $k_{ads} = S\bar{c}/4$. This adsorbed surface species then either enters the liquid (k_{sol}) or desorbs (k_{des}) from the surface. Evaporation of the species out of the bulk liquid is taken into account separately, via the term Γ_{sol} in eq 3. Solving the rate equations for the process leads to[22]

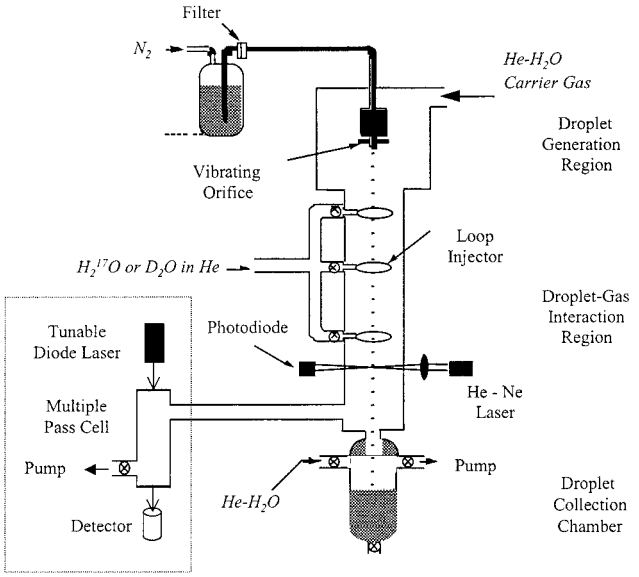

Figure 1. Schematic of droplet train flow reactor apparatus. Description is found in the text.

$$\frac{\alpha}{S - \alpha} = \frac{k_{sol}}{k_{des}} \quad (7)$$

Note that this formulation of mass accommodation differs somewhat from analogous discussions of gas sticking on ice surfaces.[31]

In D_2O uptake experiments, interfacial D−H isotope exchange opens a new channel for the disappearance of the gas-phase species. In this case, two factors are responsible for the measured disappearance of the gas-phase species:[32] (1) isotope exchange at the gas liquid interface, with probability p_{ex}, and (2) uptake into the bulk liquid of the gas-phase species that has not undergone isotope exchange, with a probability of $\alpha(1 - p_{ex})$.

The D_2O molecules that enter the bulk liquid without isotope exchange at the surface are subject to isotope exchange within the liquid. This process does not add to the measured disappearance of D_2O(g) because it is taken into account by the mass accommodation coefficient. Isotope exchange within the bulk liquid is expected to be sufficiently rapid so that evaporation of D_2O out of the liquid is negligible. Therefore, $1/\Gamma_{sol} = 0$, and for D_2O, as shown in ref 32, γ_{meas} is given by

$$\frac{1}{\gamma_{meas}} = \frac{1}{\Gamma_{diff}} + \frac{1}{\alpha(1 - p_{ex}) + p_{ex}} \quad (8)$$

Experimental Description

In the droplet train apparatus shown in Figure 1,[22,27] a fast-moving monodisperse, spatially collimated train of droplets is produced by forcing a liquid through a vibrating orifice located in a separate chamber. The number of droplets produced per second is determined by the frequency applied to the piezo ceramic that drives the orifice. Droplet formation frequencies range from 8 to 60 kHz. Depending on the pressure of the gas forcing the liquid through the orifice and the orifice diameter, the speed of the water droplets is in the range of 1600−4400 cm s^{-1}. The droplet train is passed through a ∼30 cm long, 1.4 cm in diameter, longitudinal low pressure (6−20 Torr) flow reactor that contains the trace gas species, in this case $H_2{}^{17}O$ or D_2O at a number density between 2×10^{13} and 2×10^{14} cm^{-3}

(6×10^{-4} and 6×10^{-3} Torr). The trace gas is entrained in a flowing mixture of an inert gas (usually helium) and water vapor at equilibrium pressure with the water droplets. Depending on experimental conditions, the gas volume flow rate is in the range of 80−600 $cm^3\ s^{-1}$ corresponding to a linear speed of 50−400 $cm\ s^{-1}$. The flowing carrier gases are introduced at the entrance of the reactor. The flowing trace gas is introduced through one of the three loop injectors located along the flow tube. By selecting the gas inlet port and the droplet velocity, the gas-droplet interaction time can be varied between about 2 and 15 ms.

Orifices of two diameters 28 and 64 μm were used in these studies. Depending on the frequency of orifice vibration and the liquid flow rate, these orifices generate droplets in the range of 70−130 μm and 150−300 μm in diameter, respectively. Note that these droplets are large enough that their curvature has a negligible effect on surface properties. The uniformity of the droplets and droplet speed along the flow tube are monitored with cylindrically focused He−Ne laser beams passing through the droplet train at three heights along the flow tube.[29] (For simplicity, only one beam is shown in Figure 1.) The shape and timing of the signals produced by the droplets passing through the beams provide the required information. The droplet speed along the flow tube is measured to be constant to within 3%.

For a given liquid flow rate through the droplet forming orifice, the number of droplets produced per second and their diameter (area) is determined by the frequency applied to the piezo ceramic that drives the orifice. The droplet size, and hence the total surface area of the droplets passing through the flow tube and in contact with the trace gas, is changed stepwise by cyclically switching the driving frequency between two values (switching period from 4 to 6 sec). As shown in Figure 1, the density of the trace isotopically labeled water vapor is monitored by absorption spectroscopy with a midinfrared tunable diode laser as the light source. The absorption signal is obtained by sweep integrating absorption lines at 1632.1667 cm^{-1} for $H_2{}^{17}O$[33] and 1239.0457 cm^{-1} for D_2O.[34] The uptake coefficient (γ_{meas}) as defined by eq 2 is calculated from the measured change (Δn_g) in trace gas signal via eq 9:[27]

$$\gamma_{meas} = \frac{4F_g}{\bar{c}\,\Delta A} \ln\frac{n_g}{n_g} \qquad (9)$$

Here F_g is the carrier-gas volume rate of flow through the system, $\Delta A = A_1 - A_2$ is the change in the total droplet surface area in contact with the trace gas, resulting from the switching of the droplet formation frequency. The trace gas densities n_g and n_g are the densities at the outlet of the flow tube after exposure to droplets of area A_2 and A_1, respectively, ($n_g = n_g + \Delta n_g$). In most experimental runs, A_2 and A_1 were set so that $\Delta n/n$ was in the range of 10−20%. However, to check linearity, $\Delta n/n$ was varied from 2% to 50%.

An important aspect of the experimental technique is the careful control of all the conditions within the apparatus, especially the water vapor pressure in the droplet generation chamber and in the flow tube. The near-surface temperature of the droplets is determined by the partial pressure of the water vapor in this region of droplet passage.[27] The water vapor pressure in the interaction zone was set between 1.44 and 7.51 Torr corresponding to droplet surface temperatures between 258 and 280 K, respectively. The lower temperatures, below 273 K, are obtained by evaporatively cooling the droplets which are supercooled but not frozen. The liquid delivery lines are cooled to reduce the amount of evaporative cooling necessary to reach the desired final droplet temperature. Inert carrier gas (typically helium) is added to the vapor at a partial pressure of about 3−6 Torr. Change in the overall pressure in the flow tube due to the switching of the droplet size is checked by monitoring simultaneously both the trace isotopic water vapor species studied and the concentration of an inert reference gas, in this case CH_4. The concentration of CH_4 is comparable to that of the isotopic water vapor. Because CH_4 is effectively insoluble in the water droplets, the change in the CH_4 density signal, as the droplet size is switched, measures the overall density change in the flow tube. In the course of the experiment, as the droplet area is changed from A_1 to A_2, the density of CH_4 changes by a fraction less than 10^{-3}.[35]

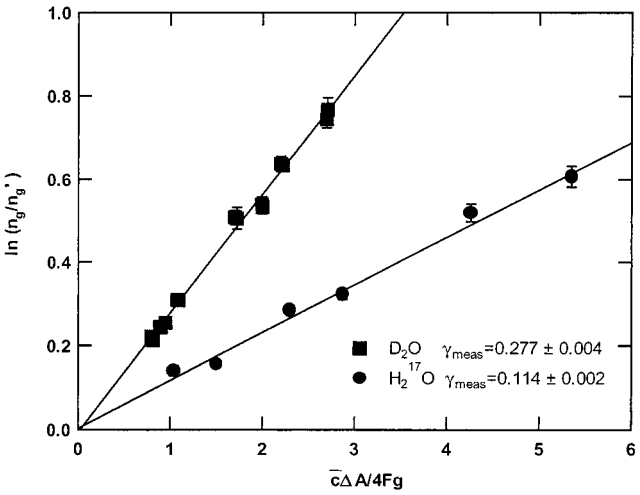

Figure 2. Experimental data showing plots of $\ln(n_g/n_g')$ as a function of $\bar{c}\Delta A/4F_g$ for $H_2{}^{17}O$ and D_2O at droplet temperature $T_d = 273$ K. Solid lines are the least-squares fit to the data. The slope of the lines is γ_{meas}. Terms are defined in the text.

The mass accommodation coefficient for $H_2O(g)$ on water is determined from the uptake of the isotope $H_2{}^{17}O$ (g).[36] The natural abundance of ^{17}O is 10^{-4}. Therefore, the $H_2{}^{17}O(g)$ in the equilibrium water vapor is in the range of 2×10^{13} to 10^{14} cm^{-3} depending on temperature (i.e., the equilibrium water vapor pressure). The controlled trace $H_2{}^{17}O(g)$ is added on top of this background, in most experiments at a density of 8×10^{13} cm^{-3} (2.5×10^{-3} Torr), which is in the range of 10^{-3} of the total water vapor pressure. The background is monitored and is taken into account in calculating γ_{meas}. The treatment of the background $H_2{}^{17}O(g)$ was checked by varying the density of the added trace gas by a factor of 10. The value of γ_{meas} was found to be constant to within the 7% scatter in the data. Still, the background $H_2{}^{17}O(g)$ limits the accuracy of the experiments and confines the uptake study to temperatures below 280 K. In the isotope exchange experiments with D_2O, the natural abundance of the isotope can be neglected because it is on the order of 10^{-7}.

A key point to note is that, although the density of $H_2{}^{17}O(g)$ changes by 10−20% as the droplet area in the flow tube is changed, the overall water vapor pressure changes by less than a factor of 10^{-3}. The trace gas water-vapor uptake is therefore measured without perturbing the liquid−vapor equilibrium. Furthermore, as described below, measurements can be conducted to separate the factors affecting gas uptake.

Results and Analysis

Figure 2 presents $\ln(n_g/n_g')$ for $H_2{}^{17}O$ and D_2O as a function of $\bar{c}\Delta A/4F_g$ at 273 K. Here, $\bar{c}\Delta A/4F_g$ was varied by changing

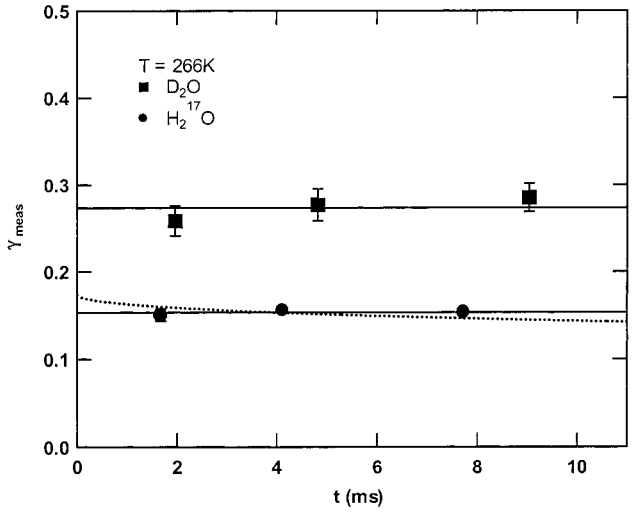

Figure 3. Uptake coefficient γ_{meas} for $H_2{}^{17}O$ and D_2O as a function of gas−liquid contact time at droplet temperature $T_d = 266$ K. Solid lines are best straight-line fits to the data. Dotted line is the best fit to H_2O data with Γ_{sol} for H_2O as defined in eq 4.

the gas flow rate and/or the droplet surface area (ΔA). Each point is the average of at least 10 area change cycles, and the error bars represent one standard deviation from the mean in the experimental $\Delta n/n$ value. As is evident in eq 9, the slope of the plots in Figure 2 yields the value of γ_{meas}, in this case with a precision of ~2%. These data yield $\gamma_{meas} = 0.114$ for $H_2{}^{17}O$ and 0.277 for D_2O. Similar plots were obtained for a wide range of experimental conditions, for which the uptake fraction, $\Delta n/n$, varied from 2 to 50%.

In Figure 3, γ_{meas} is plotted as a function of gas-droplet contact time for $H_2{}^{17}O$ and D_2O. The solid line is the best fit of the data to a straight line. The dotted line is the best fit to the experimental values of γ_{meas} including Γ_{sol} as calculated from eq 4. The value of H used is $H = 1.55 \times 10^4$ M atm^{-1} at 266 K, obtained from eq 5. Inclusion of Γ_{sol} in the data analysis increases α by about 10%. However, as is evident from Figure 3, time dependence is not discernible in the measured uptake during the gas−liquid interaction time of the experiment. Although within experimental accuracy this is consistent with eq 4, the experimental data in Figure 3 (as well as the time dependent uptake measurement at the other temperatures studied) do not provide a quantitative validation of eq 4. In view of the uncertainty of the H value to be used in eq 4 discussed earlier, it is not clear whether inclusion of Γ_{sol} would improve or worsen the accuracy of α. Therefore, we decided to neglect Γ_{sol} in the data analysis. As expected, the uptake of D_2O shows no measurable time dependence because of the essentially irreversible isotope exchange $D_2O + H_2O \rightarrow 2DOH$.

In these studies, uptake was measured at the lowest background pressure consistent with the required equilibrium vapor pressure of droplets and the necessary inert carrier gas flow. To determine the effect of gas-phase diffusive transport, the uptake was then measured as a function of increasing inert gas background pressure and with different inert gases. As noted, droplet forming orifices of two diameters were used (28 and 64 μm), generating droplet diameters ranging from 70 to 300 μm. This process allowed a change in the Knudsen number by a factor of 10. The uptake coefficients γ_{meas} for D_2O and for $H_2{}^{17}O$ at 273 K as a function of Kn are shown in Figure 4. For D_2O, γ_{meas} is independent of temperature, in the range of 265−280 K. The solid lines are best fits to the data via eq 3 for $H_2{}^{17}O$ and eq 8 for D_2O, with Γ_{diff} given by eq 6. As is evident, our formulation of gas-phase diffusion provides a good fit to

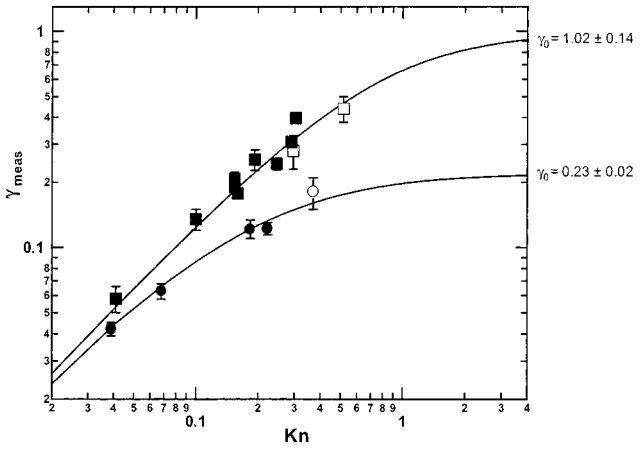

Figure 4. Uptake coefficient γ_{meas} as a function of Knudsen number (Kn) for $H_2{}^{17}O$ at 273 K (circles) and for D_2O in the temperature range of 265−280 K (squares). Open symbols were obtained with the 28 μm orifice; filled symbols with the 64 μm orifice.

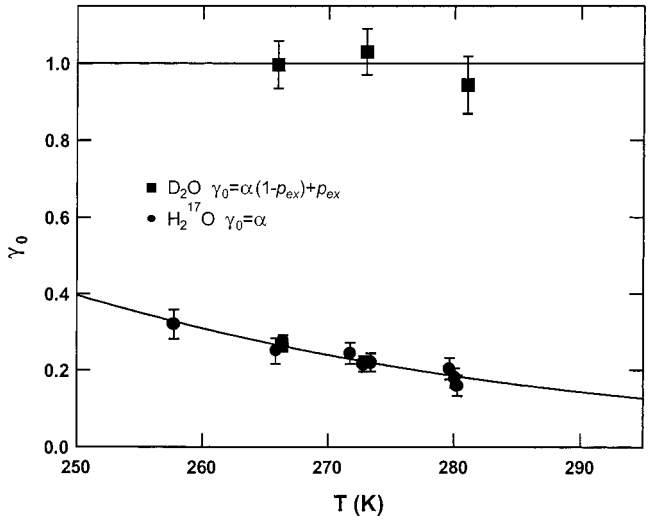

Figure 5. Mass accommodation coefficients (α) for H_2O (g) and uptake coefficient γ_o for D_2O as a function of temperature. The solid line is obtained via eq 11 with $\Delta H_{obs} = -4.8 \pm 0.5$ kcal/mol and $\Delta S_{obs} = -20.3 \pm 1.8$ cal/(mol K).

the experimental data. In previous studies, experiments were conducted with sulfuric acid and organic liquid droplets, where the effects of the liquid droplet vapor pressures on the gas-phase diffusion were negligible.[28,29] In those experiments, the validity of this formulation was demonstrated up to $Kn = 4$.

In Figure 4, the asymptote at large Kn, designated as γ_o, is the uptake coefficient in the limit of "zero pressure", i.e., in the absence of gas-phase diffusion limitation. As is evident from eq 3, for $H_2{}^{17}O$, γ_o is α, which in this case, at 273 K, is 0.23 ± 0.02. Additional Kn plots yield α for H_2O(g) on water as a function of temperature. For D_2O, the γ_o asymptote in Figure 4 is $[\alpha(1 - p_{ex}) + p_{ex}]$. The parameter γ_o as a function of temperature is plotted in Figure 5 for both H_2O and D_2O. For D_2O, $\gamma_o = [\alpha(1 - p_{ex}) + p_{ex}]$ is independent of temperature and is equal to 1 ± 0.13. With $\alpha \neq 1$, this implies that $p_{ex} = 1$.

Discussion

The thermal accommodation coefficient (S) was not measured directly. However, the measured value for the isotope exchange probability $p_{ex} = 1$, implies that every D_2O (or H_2O) molecule that strikes the surface interacts strongly with other surface

molecules. Such a strong interaction is required to promote the processes that control D/H isotope exchange.[32] Molecular interactions that can promote isotope exchange are expected to be also effective thermalizing the species. Therefore, we suggest that $p_{ex} = 1$ indicates that the thermal accommodation coefficient S is likewise unity. This result is consistent with some of the previous measurements of S for water.[18,19] The value of $S = 1$ is also consistent with molecular beam scattering studies, which show that for molecules colliding at low energies with low vapor pressure hydrogen bonding liquids such as glycerol or sulfuric acid the thermal accommodation coefficient is unity.[37,38]

The large measured value of $p_{ex} = 1$ on neutral water is surprising.[39] In bulk liquid water, D−H isotope exchange is expected to proceed mainly via proton transfer. Proton-transfer reactions in both liquid and gas-phase water are rapid in the presence of sufficient ionic concentration.[40,41] However, the ion concentration at pH ∼ 7 is far too low to account for the high observed isotope exchange probability, on the time scale of expected species surface residence time (on the order 10^{-9} s). The rate of direct hydrogen exchange in bulk water is also slow. To our knowledge, it has not been determined experimentally. However, recent calculations for small, isolated, cyclic water clusters indicate that intramolecular proton transfer occurs on the time scale of seconds.[42] Therefore, it appears that the high D−H isotope exchange probability measured in this work is an interfacial phenomenon, most likely involving highly reactive dangling OH bonds at the water surface. We are continuing to study this process.

As is shown in Figure 5, the mass accommodation coefficient for water increases from 0.17 ± 0.03 at 280 K to 0.32 ± 0.04 at 258 K. Such a negative temperature dependence for α was observed in our previous uptake studies conducted with thirty or so hydrophilic gas-phase species including alcohols, hydrogen peroxide, and acetone. With $S = 1$, following eq 7, the mass accommodation coefficient can be expressed as[43]

$$\frac{\alpha}{1-\alpha} = \frac{k_{sol}}{k_{des}} = \frac{\exp\left(\frac{-\Delta G_{sol}}{RT}\right)}{\exp\left(\frac{-\Delta G_{des}}{RT}\right)} = \exp\left(\frac{-\Delta G_{obs}}{RT}\right) \quad (10)$$

The parameter $\Delta G_{obs} = \Delta H_{obs} - T\Delta S_{obs}$ is the Gibbs energy of the transition state between gas phase and aqueous phase solvation. The solid line in Figure 5 is the best fit to the data of eq 10, with $\Delta H_{obs} = -4.8 \pm 0.5$ kcal/mol and $\Delta S_{obs} = -20.3 \pm 1.8$ cal/(mol K).

The functional form of ΔG_{obs} depends on the theoretical formulation of the uptake process. Therefore, the parameter ΔG_{obs} serves as a bridge between experiment and theory. At present, no ab initio theory exists to predict the mass accommodation of gaseous species on liquid surfaces. However, the patterns observed in the measured values of ΔH_{obs} and ΔS_{obs} for a wide range of molecules, led us to the formulation of a quantitative model for the uptake of gas-phase species by liquid water. The model is based on classical nucleation theory that predicts the formation of a critical trace−gas/water cluster at the gas/liquid interface and provides an explanation for the observed uptake results.[37,43]

In accord with experimental[44] and modeling studies,[45] the surface of water is envisioned as a sharp but finite transition region several molecular diameters in thickness within which the density changes from liquid phase to gas phase values. This interface is a dynamic region where small clusters or aggregates of water molecules are expected to be continually forming, falling apart, and re-forming. The driving force, as described by nucleation theory, is such that clusters smaller than a critical size (N^*) fall apart, whereas clusters larger than the critical size serve as centers for further aggregation and grow in size until they merge into the adjacent bulk liquid. In this model, gas uptake proceeds via such growth of critical clusters. The incoming gas molecule upon striking the surface becomes a loosely bound surface species which participates in the surface nucleation process. If such a molecule becomes part of a critical sized cluster, it will invariably be incorporated into the bulk liquid via cluster growth.

TABLE 1: Measured values of ΔH_{obs} and ΔS_{obs}, N^*, and α at 273 K[a]

molecule	ΔH_{obs} (kcal/mole)	ΔS_{obs} (cal/(mole K)	N^*	α (273 K)
acetone	−12.7	−53.7	3	0.026
methanol	−8.0	−34.9	2.3	0.056
ethylene glycol	−5.3	−24.5	1.8	0.072
water vapor	−4.8	−20.3	1.7	0.22
hydrogen peroxide	−5.5	−22.5	1.8	0.23

[a] Values are from this work and from ref 37.

The ease with which an incoming gas molecule is incorporated into bulk water depends on its ability to enter the nucleation or aggregation process with water molecules at the interface. The critical cluster consists of a specific number of molecules N^* which is the sum of the trace molecule plus the additional number of water molecules required to form the critical cluster leading to growth and subsequent uptake by the bulk liquid. This number N^* required to form a critical cluster depends on the structure of the specific molecule undergoing the process of uptake. Molecules with the ability to form strong multiple hydrogen bonds with water vapor form critical clusters more easily and thus exhibit a smaller N^*. For example, a molecule with two OH groups, such as H_2O_2 or ethylene glycol, makes a larger contribution toward the formation of a critical cluster configuration than a simple alcohol with only one OH. The critical cluster size N^* for ethylene glycol is therefore expected to be smaller than N^* for a simple alcohol. Consequently, a critical cluster is more readily formed around the former than the latter.

The values for ΔH_{obs} and ΔS_{obs} measured in the present study follow the pattern observed in previous uptake studies on liquid water, indicating that the clustering mechanism for mass accommodation applies to water vapor itself. Table 1 displays measured values of ΔH_{obs} and ΔS_{obs}, N^*, and α at 273 K for selected small molecules. The parameters for water vapor indicate that the nucleation ability of a water molecule at the liquid surface is similar to that of ethylene glycol and H_2O_2, as expected because each species can form two strong hydrogen bonds. The parameters for these species are all distinctly different from those for acetone and methanol, which can only form single hydrogen bonds. Molecular dynamics simulations of mass accommodation have so far not been able to reproduce the experimental observations,[46,47] possibly because they do not take into account correctly the hydrogen bonding dynamics of interfacial clusters.

By detailed balance, evaporation of a water molecule is the reverse of mass accommodation. Thus, according to our model, the evaporation of water molecules begins with the spontaneous emergence of a critical water cluster from the bulk liquid. The cluster dissociates into relatively weakly bound surface species, and some of these surface species leave the surface.

Atmospheric Implications

The mass accommodation coefficient for water vapor plays a role in determining the rate of water uptake by cloud droplets.[1−4] In cooling air parcels with the potential for cloud formation, slower transfer of water vapor into existing aqueous aerosol particles due to lower values of α will allow higher water vapor supersaturations to build-up. Higher supersaturation levels lead to the activation of a greater fraction of available aerosol particles, producing more, but smaller, cloud droplets than would have occurred with a larger value of α. This difference in the number and size distribution of droplets strongly affects both cloud stability against precipitation and cloud light scattering properties, modifying the influence of clouds on both meteorology and climate.[1−7]

A larger mass accommodation coefficient does not always imply faster gas-to-liquid mass transport. The mass accommodation coefficient controls the condensation growth rate when α is smaller than Γ_{diff} (see eq 3). For α in the 0.1−0.3 range, this condition applies to liquid particles smaller that $\sim$1 μm (as calculated via eq 6). Model calculations of ambient aerosol activation to cloud droplets show that the computed fraction of aerosol particles activated is very sensitive to assumed values of α below 0.1 but is relatively insensitive to values above.[48,49] Our measurements, firmly establishing that α for water vapor condensation exceeds 0.1 for typical temperatures characterizing tropospheric clouds, are an important contribution to cloud physics modeling. They support cloud physics modeling studies indicating that it is unlikely for α to be less than 0.1.[3,50,51] However, because α is greater than 0.1, the precise values determined here are not required for simulating the activation of cloud droplets in clean air by normal inorganic aqueous aerosol particles.

Laboratory studies show that droplet growth rates are very sensitive to contamination (see ref 14 and references therein). Although organic species acting as surfactants are the most likely contaminants, direct experiments have failed to demonstrate clearly that organic coatings inhibit particle growth.[52,53] This suggests that future studies should investigate the influence of common atmospheric organic pollutants (both in aerosol and gas phase) on α for aqueous surfaces.

Acknowledgment. Funding for this work was provided by the National Science Foundation Grant Nos. ATM-99-05551 and CH-0089147, by the Department of Energy Grant No. DE-FG02-98ER62581, and by the U.S.−Israel Binational Science Foundation Grant No. 1999134. Helpful discussions with J.I. Brauman, J.H. Seinfeld, A. Nenes, and G.M. Nathanson are gratefully acknowledged. We also appreciate the very helpful comments of J.G. Hudson.

References and Notes

(1) Chuang, P. Y.; Charlson, R. J.; Seinfeld, J. H. *Nature* **1997**, *390*, 594.

(2) Hudson, J. G.; Yum, S. S. *J. Atmos. Sci*. **1997**, *54*, 2642.

(3) Yum, S. S.; Hudson, J. G.; Xie, Y. *J. Geophys. Res.* **1998**, *103*, 16625.

(4) Nenes, A.; Ghan, S.; Abdul-Razak, H.; Chuang, P. Y.; Seinfeld, J. H. *Tellus, B* **2001**, *53*, 133.

(5) Charlson, R. J.; Schwartz, S. E.; Hales, J. M.; Cess, R. D.; Coakley, J. A., Jr.; Hansen, J. E.; Hoffman, D. J. *Science* **1992**, *255*, 423.

(6) *Intergovernmental Panel on Climate Change, Climate Change 2001: The Scientific Basis*; Watson, R. T., et al., Eds.; Cambridge University Press: Cambridge, U.K., 2001.

(7) Rosenfeld, D. *Science* **2000**, *287*, 1793.

(8) Rideal, E. *J. Phys. Chem*. **1925**, *29*, 1585.

(9) Cammenga, H. K. In *Current Topics in Materials Science*; Kaldis, Ed.; North-Holland Publishing Company: 1980; Vol. 5, pp 335−446.

(10) Wagner, P. E. *Aerosol Microphysics II*; Marlow, W. H., Ed.; Springer-Verlag: Duesseldorf, Germany, 1982; pp 129−178.

(11) Mozurkewich, M. *Aerosol Sci. Technol*. **1986**, *5*, 223.

(12) Garnier, J. P.; Ehrhard, Ph.; Mirabel, Ph. *Atmos. Res*. **1987**, *21*, 41.

(13) Beloded, V. V.; Kirichewskij, G. A.; Nuzhnyj, V. M. *J. Aerosol Sci*. **1989**, *20*, 1047.

(14) Hagen, D. E.; Schmitt, J.; Trueblood, M.; Carstens, J. *J. Atmos. Sci*. **1989**, *46*, 803.

(15) Maerefat, M.; Akmatasu, T.; Fujikawa, S. *Exp. Fluids* **1990**, *9*, 345.

(16) Shaw, R. A.; Lamb, D. *J. Chem. Phys*. **1999**, *111*, 10659.

(17) Zagaynov, V. A.; Nuzhny, V. M.; Cheeusova, T. A.; Lushnikov, A. A. *J. Aerosol Sci.* **2000**, *31*, Suppl. 1, S795.

(18) Alty, T.; Mackay, C. A. *Proc. R. Soc*. **1935**, *A149*, 104.

(19) Sageev, G.; Flagan, R. C.; Seinfeld, J. H.; Arnold, S. *J. Colloid Interface Sci*. **1986**, *113*, 421.

(20) Chodes, N.; Warner, J.; Gagin, A. *J. Atmos. Sci*. **1974**, *31*, 1351.

(21) Kolb, C. E.; Davidovits, P.; Worsnop, D. R.; Shi, Q.; Jayne, J. T. Manuscript submitted to *Prog. React. Kinet. Mech*.

(22) Shi, Q.; Davidovits, P.; Jayne, J. T.; Worsnop, D. R.; Kolb, C. E. *J. Phys. Chem. A* **1999**, *103*, 8812.

(23) Fuchs, N. A.; Sutugin, A. G. *Highly Dispersed Aerosols*; Ann Arbor Science Publishers: Newton, MA, 1970.

(24) Widmann, J. F.; Davis, E. J. *J. Aerosol Sci*. **1997**, *28*, 87.

(25) Seinfeld, J. H.; Pandis, S. N. *Atmospheric Chemistry and Physics*; John Wiley & Sons: New York, 1998; p 602.

(26) Hanson, D. R.; Ravishankara, A. R.; Lovejoy, E. R. *J. Geophys. Res.* **1996**, *101*, 9063.

(27) Worsnop, D. R.; Zahniser, M. S.; Kolb, C. E.; Gardner, J. A.; Watson, L. R.; Van Doren, J. M.; Jayne, J. T.; Davidovits, P. *J. Phys. Chem*. **1989**, *93*, 1159.

(28) Swartz, E.; Shi, Q.; Davidovits, P.; Jayne, J. T.; Worsnop, D. R.; Kolb, C. E. *J. Phys. Chem. A* **1999**, *103*, 8824.

(29) Worsnop, D. R.; Shi, Q.; Jayne, J. T.; Kolb, C. E.; Swartz, E.; Davidovits, P. *J. Aerosol Sci*. **2001**, *32*, 877.

(30) Jayne, J. T.; Duan, S. X.; Davidovits, P.; Worsnop, D. R.; Zahniser, M. S.; Kolb, C. E. *J. Phys. Chem*. **1991**, *95*, 6329.

(31) For water condensing on ice surfaces, Brown et al. (*J. Phys. Chem.* **1996**, *100*, 4988) have formulated uptake in terms of a sticking coefficient *S* and a condensation coefficient α, which need to be distinguished from the definitions used here. Their *S* does not distinguish thermal and mass accommodation; that is, they assume that thermal accommodation leads to crystalline ice growth. Their formulation of α is equivalent to γ_{meas} in eq 3; that is, their α represents net uptake after accounting for evaporation from the ice surface. Underlying these differences in definition is the role of dissolution in the bulk condensed phase, which is not included in the case of ice but is represented by k_{sol} for accommodation into the liquid (as well as the diffusion-limited uptake into the bulk liquid represented by Γ_{sol}).

(32) Shi, Q.; Li, Y. Q.; Davidovits, P.; Jayne, J. T.; Worsnop, D. R.; Mozurkewich, M.; Kolb, C. E. *J. Phys. Chem. B* **1999**, *103*, 2417.

(33) Rothman, L. S.; Rinsland, C. O.; Goldman, A.; Massie, S. T.; Edward, D. P.; Flaud, J. M.; Perrin, A.; Camy-Peyret, C.; Dana, V.; Mandin, J. V.; Schroeder, J.; Mccann, A.; Gamache, R. R.; Wattson, R. B.; Yoshino, K.; Chance, K. V.; Jucks, K. W.; Brown, L. R.; Nemtchinov, V.; Varanasi, P. *J. Quantum Spectrosc. Radiat. Transfer* **1998**, *60*, 665.

(34) Camy-Peyret, C.; Flaud, J. M.; Mahmoudi, A. *Int. J. Infrared Millimeter Waves* **1985**, *6*, 199.

(35) The reference gas, in this case CH_4, is chosen to have diffusion properties similar to the trace gas studied. Any change in the reference gas concentration with droplet switching determines the "zero" of the system and is subtracted from observed changes in trace gas concentration. In the present experiments, this correction was always less than 5%.

(36) The chemical properties that are likely to affect mass accommodation of an H_2O molecule, such as the strength of hydrogen bonding, do not change with oxygen isotope substitution. Therefore, α is expected to be independent of the H_2O oxygen isotope composition.

(37) Nathanson, G. M.; Davidovits, P.; Worsnop, D. R.; Kolb, C. E. *J. Phys. Chem*. **1996**, *100*, 13007.

(38) Saecker, M. E.; Nathanson, G. M. *J. Chem. Phys*. **1993**, *99*, 7056.

(39) Isotope exchange on neutral water was also observed in experiments with deuterated ethanol.[32] For near-neutral water, between pH = 5 and 9, p_{ex} is about 0.04. The isotope exchange probability increases both toward low and high pH and levels off to a plateau of about 0.15 at pH 2 and 12, respectively.

(40) Lux, Z.; Meiboom, S. *J. Am. Chem. Soc*. **1964**, *86*, 4768.

(41) Smith, D.; Adams, N. G.; Henchman, M. J. *J. Chem. Phys*. **1980**, *72*, 4951.

(42) Loerting, T.; Liedl, K. R.; Rode, B. M. *J. Chem. Phys*. **1998**, *109*, 2672.

(43) Davidovits, P.; Jayne, J. T.; Duan, S. X.; Worsnop, D. R.; Zahniser, M. S.; Kolb, C. E. *J. Phys. Chem*. **1991**, *95*, 6337.

(44) Braslau, A.; Pershan, P. S.; Swislow, G.; Ocko, B. M.; Als-Nielsen, *J. Phys. Rev*. **1988**, *A38*, 2457.

(45) Taylor, R. S.; Dang, L. X.; Garrett, B. C. *J. Phys. Chem*. **1996**, *100*, 11720 and references therein.
(46) Wilson, M. A.; Pohorille, A. *J. Phys. Chem. B* **1997**, *101*, 3130.
(47) Taylor, R. S.; Ray, D.; Garrett, B. C. *J. Phys. Chem. B* **1997**, *101*, 5473.
(48) In response to this work, A. Nenes and J. H. Seinfeld have calculated the effect of the water vapor mass accommodation coefficient on nonequilibrium cloud droplet formation in an adiabatic air parcel rising at 0.5 m/s with trimodal ammonium sulfate aerosol number densities characteristic of both clean marine and polluted urban atmospheres. In both cases, as the assumed value of α was varied from 0.001 to 0.01 and to 0.1, the computed fraction of aerosol particles activated to cloud droplets decreased dramatically. However, as α was increased from 0.1 to 1.0, spanning the values reported here, the decrease in the fraction of particles activated was modest.
(49) Fukuta, N.; Walter, L. A. *J. Atmos. Sci*. **1970**, *27*, 1160.
(50) Leaitch, W. R.; Strapp, J. W.; Isaac, G. A.; Hudson, J. G. *Tellus* **1986**, *388*, 328.
(51) Hudson, J. G.; Garret, T. J.; Hobbs, P. V.; Strader, S. R.; Xie, Y. X.; Yum, S. S. *J. Atmos. Sci*. **2000**, *57*, 2696.
(52) Cruz, C. N.; Pandis, S. N. *J. Geophys. Res*. **1998**, *103*, 13111.
(53) Hansson, H.-C.; Rood, M. J.; Koloutsou-Vakakis, S.; Hameri, K.; Orsini, D.; Wiedensohler, A. *J. Atmos. Chem*. **1998**, *31*, 321.